

1 **The role of lineage, hemilineage and temporal identity in establishing neuronal targeting and**  
2 **connectivity in the *Drosophila* embryo**

3  
4  
5 Brandon Mark<sup>1</sup>, Sen-Lin Lai<sup>1</sup>, Aref Arzan Zarin<sup>1</sup>, Laurina Manning<sup>1</sup>, Albert Cardona<sup>2</sup>, James W. Truman<sup>2,3</sup>,  
6 and Chris Q. Doe<sup>1\*</sup>

7  
8 <sup>1</sup>Institute of Neuroscience, Institute of Molecular Biology, Howard Hughes Medical Institute, University of  
9 Oregon, Eugene, OR 97403

10 <sup>2</sup>Janelia Research Campus, Howard Hughes Medical Institute, Ashburn, VA 20147

11 <sup>3</sup>Friday Harbor Laboratories, University of Washington. Friday Harbor, WA 98250

12  
13  
14  
15 \* Author for correspondence at [cdoe@uoregon.edu](mailto:cdoe@uoregon.edu)

16  
17 Key words: neuroblast, hemilineage, temporal identity, pathfinding, cell lineage, neural circuits

18  
19  
20 **Abstract**

21  
22 The mechanisms specifying neuronal diversity are well-characterized, yet it remains unclear how these  
23 mechanisms are used to establish neuronal morphology and connectivity. Here we map the developmental  
24 origin of over 78 neurons from seven identified neural progenitors (neuroblasts) within a complete TEM  
25 reconstruction of the *Drosophila* larval CNS. This allowed us to correlate developmental mechanism with  
26 neuronal projection and synapse targeting. We find that clonally-related neurons from individual neuroblasts  
27 project widely in the neuropil without preferential circuit formation. In contrast, the two Notch<sup>ON</sup>/Notch<sup>OFF</sup>  
28 hemilineages from each neuroblast project to restricted dorsal/motor neuropil domains (Notch<sup>ON</sup>) and  
29 ventral/sensory neuropil domains (Notch<sup>OFF</sup>). Thus, each neuroblast contributes both motor and sensory  
30 processing neurons, although they share little connectivity. Lineage-specific constitutive Notch transforms  
31 sensory to motor hemilineages, showing hemilineage identity determines neuronal targeting. Within a  
32 hemilineage, neurons of different temporal cohorts target their synapses to different sub-domains of the  
33 neuropil. Importantly, neurons sharing a sub-domain defined by hemilineage and temporal identity  
34 preferentially connect to neurons of another hemilineage/temporal profile. We propose that the mechanisms  
35 that generate neural diversity are also determinants of neural circuit formation.

36

## 37 Introduction

38  
39 Tremendous progress has been made in understanding the molecular mechanisms generating neuronal  
40 diversity in both vertebrate and invertebrate model systems. In mammals, spatial cues generate distinct pools  
41 of progenitors which generate a diversity of neurons and glia appropriate for each spatial domain (1). The  
42 same process occurs in invertebrates like *Drosophila*, but with a smaller number of cells, and this process is  
43 particularly well-understood. Spatial patterning genes act combinatorially to establish single, unique  
44 progenitor (neuroblast) identity; these patterning genes include the dorsoventral columnar genes *vnd*, *ind*, *msb*  
45 (2-4) and the orthogonally expressed *wingless*, *hedgehog*, *gooseberry*, and *engrailed* genes (5-8). These factors endow  
46 each neuroblast with a unique spatial identity, the first step in generating neuronal diversity (Figure 1A, left).  
47 The second step occurs as each neuroblast “buds off” a series of ganglion mother cells (GMCs) which  
48 acquire a unique identity based on their birth-order, due to inheritance from the neuroblast of a “temporal  
49 transcription factor”– Hunchback (Hb), Krüppel (Kr), Pdm, and Castor (Cas) – which are sequentially  
50 expressed by nearly all embryonic neuroblasts (9). The combination of spatial and temporal factors leads to  
51 the production of a unique GMC with each neuroblast division (Figure 1A, middle). The third and final step  
52 in generating neuronal diversity is the asymmetric division of each GMC into a pair of post-mitotic neurons;  
53 during this division, the Notch inhibitor Numb (Nb) is partitioned into one neuron (Notch<sup>OFF</sup> neuron)  
54 whereas the other sibling neuron receives active Notch signaling (Notch<sup>ON</sup> neuron), thereby establishing two  
55 distinct hemilineages (10-13)(Figure 1A, right). In summary, three developmental mechanisms generate  
56 neuronal diversity within the embryonic CNS: neuroblast spatial identity, GMC temporal identity, and  
57 neuronal hemilineage identity.

58 A great deal of progress has also been made in understanding neural circuit formation in both vertebrates  
59 and invertebrate model systems, revealing a multi-step mechanism. Mammalian neurons initially target their  
60 axons to broad regions (e.g. thalamus/cortex), followed by targeting to a neuropil domain (glomeruli/layer),  
61 and finally forming highly specific synapses within the targeted domain (reviewed in 14).

62 Despite the progress in understanding the generation of neuronal diversity and the mechanisms  
63 governing axon guidance and neuropil targeting, how these two developmental processes are related remains  
64 unknown. While it is accepted that the identity of a neuron is tightly linked to its connectivity, the  
65 developmental mechanisms involved remain unclear. For example, do clonally-related neurons target similar  
66 regions of the neuropil due to the expression of similar guidance cues? Do temporal cohorts born at similar  
67 times show preferential connectivity? Are neurons expressing the same transcription factor preferentially  
68 interconnected? It may be that lineage, hemilineage, and temporal factors have independent roles in circuit  
69 formation; or that some mechanisms are used at different steps in circuit assembly; or that mechanisms used  
70 to generate neural diversity could be independent of those regulating circuit formation. Here we map  
71 neuronal developmental origin, neuropil targeting, and neuronal connectivity within a whole CNS TEM  
72 reconstruction (15). This provides us the unprecedented ability to identify correlations between development  
73 and circuit formation – at the level of single neurons/single synapses – and test those relationships to gain  
74 insight into how mechanisms known to generate diversity might be coupled to mechanisms of neural circuit  
75 formation. We find that lineage, hemilineage, and temporal identity are all strongly correlated with features of  
76 neuronal targeting that directly relate to establishing neural circuits.

## 77 Results

### 78 Clonally related neurons project widely within the neuropil

82 It is not possible to determine the clonal relationship of neurons in the TEM volume based on anatomical  
83 features alone; for example, clonally-related neurons are not ensheathed by glia as they are in grasshopper  
84 embryos or the *Drosophila* larval brain (16, 17). We took a multi-step approach to identify clonally-related  
85 neurons in the TEM reconstruction. First, we generated sparse neuroblast clones and imaged them by light  
86 microscopy. All neuroblasts assayed had a distinctive clonal morphology including the number of fascicles  
87 entering the neuropil, cell body position, and morphology of axon/dendrite projections (Figure 1B-G; and  
88 data not shown). The tendency for neuroblast clones to project one or two fascicles into the neuropil has also  
89 been noted for larval neuroblast clones (11-13). We assigned each clone to its parental neuroblast by  
90 comparing our clonal morphology to that seen following single neuroblast DiI labeling (18-20), and what has  
91 been reported previously for larval lineages (21, 22), as well as the position of the clone in the segment, and in  
92 some cases the presence of well-characterized individual neurons (e.g. the “looper” neurons in the NB2-1  
93 clone). Note that we purposefully generated clones after the first-born Hb+ neurons, because the Hb+  
94 neurons have cell bodies contacting the neuropil and do not fasciculate with later-born neurons in the clone,  
95 making it difficult to assign them to a specific neuroblast clone. We found that neurons in a single neuroblast  
96 clone, even without the Hb+ first-born neurons included, project widely throughout the neuropil, often  
97 targeting both dorsal motor neuropil and ventral sensory neuropil, as well as widely along the mediolateral  
98 axis of the neuropil (Figure 1B).

99 Next, we used these neuroblast lineage-specific features to identify the same clonally-related neurons in  
100 the TEM reconstruction. We identified neurons that had clustered cell bodies, clone morphology matching  
101 that seen by light microscopy (Figure 1C), and, with the exception of NB5-2 in segment A1R, one or two  
102 fascicles (Figure 1D,E). The similarity in overall clone morphology was striking (compare Figure 1B and 1C).  
103 We used two methods to validate the clonal relationship observed in the TEM reconstruction. We used  
104 neuroblast-specific Gal4 lines (13, 23) to generate MCFO labeling of single neurons, and found that in each  
105 case we could match the morphology of an MCFO-labeled single neuron from a known neuroblast to an  
106 identical single neuron in the same neuroblast clone within the TEM reconstruction (data not shown). We  
107 also showed that the TEM reconstruction had the same clone on the left and right side of abdominal segment  
108 1 (A1), where it contained a similar number of neurons (Figure 1D, bottom) and had similar clonal  
109 morphology (data not shown). Overall, we mapped seven neuroblast clones into the TEM reconstruction  
110 (Figure 1F,G). In addition, our lab and others have previously mapped most of the NB3-3 neuronal progeny  
111 in the TEM reconstruction (24, 25). Thus, we have mapped almost 1/3 of all neurons in the A1L  
112 hemisegment (78/295) (Table 1). We conclude that each neuroblast clone has stereotyped cell body  
113 positions, 1-2 fascicles entering the neuropil, and widely projecting axons and dendrites.

114

### 115 **Lineages generate two morphologically distinct classes of neurons, which project to dorsal and** 116 **ventral regions of the neuropil.**

117

118 After mapping seven lineages into the EM volume, we observed that most lineages seemed to contain two  
119 broad classes of neurons with very different projection patterns. Recent work has shown that within a larval  
120 neuroblast lineage all Notch<sup>ON</sup> neurons have a similar clonal morphology (called the Notch<sup>ON</sup> hemilineage),  
121 whereas the Notch<sup>OFF</sup> hemilineage shares a different morphology (11-13). We hypothesized that the observed  
122 morphological differences may be due to hemilineage identity (Figure 2). First, we used NBLAST (26) to  
123 compare the morphology of clonally related neurons. We observed that five of the seven neuroblast lineages  
124 generated two highly distinct candidate hemilineages that each projected to a focused domain in the dorsal or  
125 ventral neuropil (Figure 2A-D; Fig. S1). A sixth neuroblast lineage, NB7-4, generated neurons projecting to  
126 the ventral neuropil, and a pool of glia (Figure 2E). The seventh neuroblast lineage, NB3-3 (Figure 2F), has

127 previously been shown to directly generate a single Notch<sup>OFF</sup> hemilineage due to direct differentiation of the  
128 neuroblast progeny as neurons, bypassing the terminal asymmetric cell division (25, 27). Interestingly, only  
129 the ventral candidate hemilineages contained intersegmental projection neurons (Fig. S2). We conclude that  
130 NBLAST can morphologically identify candidate hemilineages, and that each neuroblast generates a  
131 hemilineage projecting to the ventral neuropil, and one projecting to the dorsal neuropil (Figure 2G).  
132 Additionally, comparing morphologies of all neurons across seven lineages showed that while neurons from  
133 the same hemilineage are morphologically related, there is no morphological relationship between neurons of  
134 two different hemilineages despite being from the same neuroblast lineage (Figure 2H) suggesting that, like  
135 the larva, hemilineages offer a mechanism by which each lineage can essentially generate two totally different  
136 classes of neurons, thus doubling the diversity generated from a single lineage. Furthermore, the NB3-3 data  
137 raises the question of whether Notch<sup>OFF</sup> hemilineages target the ventral neuropil, and Notch<sup>ON</sup> hemilineages  
138 project to the dorsal neuropil.

139

### 140 Hemilineage identity determines axon projection targeting to dorsal or ventral neuropil

141

142 We next wanted to validate the NBLAST hemilineage assignments, to determine whether Notch<sup>ON</sup>  
143 hemilineages always project to dorsal neuropil domains (and ventral neuropil for Notch<sup>OFF</sup> hemilineages), and  
144 to experimentally test whether hemilineage identity determines neuropil targeting. We can achieve all three  
145 goals by using Gal4 lines to drive expression of constitutively active Notch (Notch<sup>intra</sup>) in single neuroblast  
146 lineages to transform Notch<sup>OFF</sup> hemilineages into Notch<sup>ON</sup> hemilineages.

147 There are Gal4 lines specifically expressed in NB1-2, NB7-1, and MB7-4 (13, 28) which we used to drive  
148 Notch<sup>intra</sup> expression. Notch<sup>intra</sup> expression led to a loss of ventral projections in the NB1-2 and NB7-1  
149 lineages, with a concomitant increase in dorsal neuropil projections (Figure 3A,B). For example, Notch<sup>intra</sup>  
150 expression throughout the NB1-2 lineage increased the number of ventral contralateral projections, and  
151 eliminated all dorsal ascending/descending projections (compare insets, Figure 3A,D). Similarly, Notch<sup>intra</sup>  
152 expression in the NB7-4 lineage led to a loss of ventral projections and an increase in the number of glia  
153 (Figure 3C); the loss of ventral neurons is apparent in both posterior views (Figure 3C,F) and dorsal views  
154 (insets, Figure 3C,F). These results strongly support the NBLAST assignments of neurons into two distinct  
155 hemilineages, and show that all tested neuroblast lineages make a Notch<sup>ON</sup> hemilineage that projects to the  
156 dorsal neuropil (or makes glia), and a Notch<sup>OFF</sup> hemilineage that projects to the ventral neuropil. This is a  
157 remarkable subdivision within each hemilineage, both because of the large difference in dorsoventral position  
158 as well as the difference in functional properties. In summary, neuroblasts are likely to contribute motor  
159 neurons and premotor neurons from their Notch<sup>ON</sup> hemilineage, and post-sensory neurons from their  
160 Notch<sup>OFF</sup> hemilineage. Most importantly, we show that hemilineage identity determines neuronal targeting to  
161 specific domains of dorsal or ventral neuropil.

162

### 163 Hemilineage identity determines synapse targeting to motor or sensory neuropil domains

164

165 The observation that each lineage generates a dorsal and ventral hemilineage in a Notch dependent fashion  
166 suggests the possibility that each lineage is generating a class of neurons that project into the motor neuropil  
167 and the sensory neuropil (29-31). To confirm and expand our mapping of neuropil functional domains, we  
168 mapped the synapse position of pre-motor neurons and post-sensory neurons. We confirm previous findings  
169 (30-33) mapping the dorsal localization of motor neuron post-synaptic sites, the ventral location of sensory  
170 pre-synaptic sites, and the intermediate location of proprioceptive pre-synaptic sites (Figure 4A). Extending  
171 this analysis, we find pre-motor neurons target their post-synaptic sites to a broader dorsal neuropil territory,

172 and post-sensory neurons target their pre-synaptic sites to a broader ventral neuropil territory (Figure 4B,C)  
173 suggesting that the dorsoventral division of the neuropil into motor and sensory domains exists to the level of  
174 interneurons, and strengthens the possibility that neuroblast lineages are generating a sensory and a motor  
175 hemilineage.

176 To test this, we use the functional motor and sensory domains as landmarks to map synaptic localization  
177 for different hemilineages. We find that the dorsal hemilineages localize both pre- and post-synaptic sites to  
178 the motor neuropil, whereas ventral hemilineages localize both pre- and post-synaptic sites to the sensory  
179 neuropil (Figure 4D-G; Fig. S3), but see Discussion for caveats. Consistent with these observations, we find  
180 that the vast majority of sensory input to these neurons from these lineages is onto ventral hemilineages, and  
181 the vast majority of motor neuron input from these lineages comes from dorsal hemilineages (Figure 4H). We  
182 conclude that, at least for assayed hemilineages, Notch<sup>ON</sup> hemilineages target projections and synapses to the  
183 motor neuropil, whereas Notch<sup>OFF</sup> hemilineages target projections and synapses to the sensory neuropil  
184 (Figure 4I).

185

### 186 Hemilineages target discrete regions of the neuropil.

187

188 After showing that hemilineages target restricted domains of dorsal or ventral neuropil, we asked if individual  
189 hemilineages tile the neuropil or have overlapping domains. We mapped the pre- and post-synaptic position  
190 for six ventral hemilineages and four dorsal hemilineages (excluding the NB7-4D glial hemilineage). We find  
191 that each of the dorsal hemilineages target pre-synapses and post-synapses to distinct but overlapping regions  
192 of the neuropil (Figure 5A,C). Similarly, each of the ventral hemilineages target pre-synapses and post-  
193 synapses to distinct but overlapping regions of the neuropil (Figure 5B,D). Clustering neurons by synapse  
194 similarity (a measure of synaptic distribution similarity) confirms that most neurons in a hemilineage cluster  
195 their pre- and post-synapses within the neuropil (Figure 5E). We conclude that neuroblast hemilineages  
196 contain neurons that project to distinct but overlapping neuropil regions, strongly suggesting that the  
197 developmental information needed for neuropil targeting is shared by neurons in a hemilineage, but not by all  
198 neurons in a complete neuroblast lineage (see Discussion).

199

### 200 Mapping temporal identity in the TEM reconstruction: radial position is a proxy for neuronal birth-order

201

202 Most embryonic neuroblasts sequentially express the temporal transcription factors Hb, Kr, Pdm, and Cas  
203 with each factor inherited by the GMCs and young neurons born during each window of expression  
204 (reviewed in 34). Previous work has shown that early-born Hb<sup>+</sup> neurons are positioned in a deep layer of the  
205 cellular cortex adjacent to the developing neuropil, whereas late-born Cas<sup>+</sup> neurons are at the most  
206 superficial position, with Kr<sup>+</sup> and Pdm<sup>+</sup> neurons positioned in between (Figure 6A)(9, 35). Thus, in the late  
207 embryo, radial position can be used as a proxy for temporal identity (Figure 6B). To determine if this  
208 relationship is maintained in newly hatched larvae, we could not simply stain for Hb and Cas, as their  
209 expression is not reliably maintained in newly hatched larvae. Instead, we used more stable reporters for Hb  
210 (a recombinereed Hb:GFP transgene) and Cas (*cas-gal4* line driving *UAS-histone:RFP*). We confirm the radial  
211 position of Hb:GFP and Cas>RFP in the late embryonic CNS, and importantly, show that the same  
212 deep/superficial layering is maintained in newly hatched larvae (Figure 6C,D). Next, we identified 13 pairs of  
213 neurons shown previously to be born in the Hb<sup>+</sup> or Cas<sup>+</sup> temporal windows (Fig. S4). Additionally, we  
214 generated a new Hb-LexA construct in order to identify additional Hb<sup>+</sup> neurons, which we then traced in the  
215 EM volume (Figure 6E,F, cyan neurons). We also used *cas-gal4* to drive MCFO in order to identify new late-  
216 born neurons which we were also able to trace in the TEM volume (Figure 6E,F magenta neurons). In total,

217 we identified 18 pairs of neurons with known birthdates. In order to quantify distance from the neuropil in  
218 the EM volume, we measured the neurite length between the cell body and the neuropil entry point. We  
219 found that all confirmed Hb+ neurons were located deep in the cellular cortex, close to the neuropil, whereas  
220 late-born neurons were located superficially in the cortex (Figure 6G,H). We also located all of these neurons  
221 in both the left and right hemisegments of A1 and found that left/right homologs had extremely similar  
222 cortex neurite lengths (Figure 6I). Thus, we confirm that cortex neurite length can be used as a proxy for  
223 temporal identity, is consistent across at least two hemisegments, and thus can be used to approximate the  
224 temporal identity of any neuron in the TEM reconstruction.

225

### 226 **Temporal identity subdivides hemilineage neuropil domains**

227

228 In order to determine the role of temporal identity in neuronal targeting and connectivity we first used cortex  
229 neurite length to map the birthdates of all neurons in 10 hemilineages (Fig. S5). Unlike the striking dorsal-  
230 ventral division observed from mapping hemilineages, the synaptic distributions of individual temporal  
231 cohorts appeared far more overlapping (Fig. S5). To quantify this, we compared the synapse similarity of  
232 hemilineage-related neurons and temporal-related neurons and found that neurons related by hemilineage  
233 were more similar than those related by birthdate (Fig. S6). We conclude that hemilineages, not temporal  
234 cohorts, are more important determinants of neuropil targeting.

235 We next asked whether temporal identity subdivides each hemilineage to allow more precise “sub-  
236 regional” targeting of neuronal projections or synapses. Previous work has shown that temporal identity in  
237 NB3-3 plays a role in segregating neurons into distinct circuits (25). Early-born neurons (A08x/m) are  
238 involved in escape behaviors while late-born neurons (A08e1/2/3) are involved in proprioception (22).  
239 Interestingly, late-born NB3-3 neurons appeared to have more dorsal projections compared to early-born  
240 NB3-3 neurons, as well as project to different regions of the central brain (Figure 7A-C). We first calculated  
241 the mean cortex neurite length for all 11 pairs of neurons in NB3-3 left/right lineages, and found that in all  
242 but one case, late-born neurons all had longer cortex neurites than confirmed early-born neurons, further  
243 strengthening the use of cortex-neurite length as a birth-order proxy. We grouped the remaining neurons into  
244 temporal cohorts based on their cortex neurite lengths, and examined the spatial distribution of their pre and  
245 post-synaptic sites. Clustering of NB3-3 neurons by either pre or post-synaptic similarity found a near perfect  
246 correlation between birth-order and synapse similarity (Figure 7E,F). We conclude that the functional  
247 differences observed between temporal cohorts of NB3-3 neurons correlate with a subregionalization of pre-  
248 and post-synaptic sites.

249 We next tested whether sub-regionalization of synaptic targeting within a hemilineage by temporal  
250 cohorts is a general feature. To do this, we examined the relationship between birth-order and synaptic  
251 targeting across other hemilineages. Indeed, examination of the NB5-2 ventral hemilineage showed that early-  
252 and late-born neurons targeted their projections to “sub-regional” domains of the full hemilineage (Figure  
253 8A,B). Additionally, both pre- and post-synaptic distributions were strongly correlated with birth-order  
254 (Figure 8C-H). Similar results were observed for pre-synaptic targeting (but not post-synaptic targeting) in the  
255 NB5-2 dorsal hemilineage (Figure 8I-P). Examination of all other hemilineages in this manner found that  
256 only one hemilineage did not have a significant correlation between birth-order and presynaptic targeting  
257 (NB1-2D) and only one hemilineage did not show a significant relationship between birth-order and post-  
258 synaptic targeting (NB5-2D). Pooling data from all hemilineages shows a positive correlation between  
259 synapse location and temporal identity (Figure 8Q). We conclude that temporal identity subdivides  
260 hemilineages into smaller populations of neurons that target both projections and synapses to different sub-

261 domains within the larger hemilineage targeting domain (Figure 8R). Thus, hemilineage identity provides  
262 coarse targeting within neuropil, and temporal identity refines targeting to several smaller sub-domains.

263

## 264 Discussion

265

266 Many studies in *Drosophila* and mammals are based on the identification and characterization of clonally-  
267 related neurons, looking for common location (36, 37), identity (37, 38), or connectivity (39). Our results  
268 suggest that analyzing neuronal clones may be misleading due to the clone comprising two quite different  
269 hemilineages. For example, performing RNAseq on individual neuroblast lineages is unlikely to reveal key  
270 regulators of pathfinding or synaptic connectivity, due to the mixture of disparate neurons from two  
271 hemilineages.

272 Previous work on *Drosophila* larval neuroblasts show that the pair of hemilineages have different  
273 projection patterns and neurotransmitter expression (11-13). We extend these pioneering studies to  
274 embryonic neuroblasts, and show that pairs of hemilineages not only have different projection patterns, but  
275 also target pre- and post-synapses to distinct regions. Surprisingly, in all lineages where we performed Notch  
276 mis-expression experiments, neurons in the Notch<sup>ON</sup> hemilineage always projected to the dorsal neuropil,  
277 whereas Notch<sup>OFF</sup> neurons projected to the ventral neuropil. It is unlikely that all Notch<sup>ON</sup> hemilineages  
278 target the dorsal neuropil, however, as the NB1-1 interneuron pCC is from a Notch<sup>ON</sup> hemilineage (10) yet  
279 projects ventrally and receives strong sensory input, and its sibling aCC motor neuron is from the Notch<sup>OFF</sup>  
280 hemilineage (10) and projects dendrites in the dorsal motor neuropil. We think it is more likely that the  
281 Notch<sup>ON</sup>/Notch<sup>OFF</sup> provides a switch to allow each hemilineage to respond differently to dorsoventral  
282 guidance cues: in some cases the Notch<sup>ON</sup> hemilineage projects dorsally, and in some cases it projects  
283 ventrally. Nevertheless, our finding that neuroblasts invariably produce both sensory and motor hemilineages  
284 reveals the striking finding that the sensory and motor processing components of the neuropil are essentially  
285 being built in parallel, with one half of every GMC division contributing to either sensory or motor networks.  
286 This has not been observed in larval hemilineages, and may be the result of an evolutionary strategy to  
287 efficiently build the larval brain as fast as possible.

288 While we do observe some differences between embryonic and larval hemilineages, the similarities are far  
289 more striking. Previous work has shown that larval and embryonic hemilineages have similar morphological  
290 features (13), suggesting the possibility that these neurons could be performing analogous functions. Here we  
291 show that two components of a proprioceptor circuit, the Jaam and Saaghi neurons (24), are derived from  
292 two hemilineages of NB5-2 (also called lineage 6 (21)). Activation of either of these hemilineages in adults  
293 results in uncoordinated leg movement, consistent with the idea that these hemilineages could be involved in  
294 movement control. Similarly, adult activation of the NB3-3 lineage (also called lineage 8 (21)) caused postural  
295 effects, again consistent our previous findings that activation of this lineage in larvae cause postural defects  
296 (24). In the future, it will be interesting to further explore the functional and organizational similarities of the  
297 embryonic and larval nervous systems.

298 Our results suggest that all neurons in a hemilineage respond similarly to the global pathfinding cues that  
299 exist within the embryonic CNS. Elegant previous work showed that there are gradients of Slit and Netrin  
300 along the mediolateral axis (30), gradients of Semaphorin 2a along the dorsoventral axis (33), and gradients of  
301 Wnt5 along the anteroposterior axis (40). We would predict that the palette of receptors for these patterning  
302 cues would be shared by all neurons in a hemilineage, to allow them to target a specific neuropil domain; and  
303 different in each of the many hemilineages, to allow them to target different regions of the neuropil.  
304 Expression of constitutively-active Notch in single neuroblast lineages will make two Notch<sup>ON</sup> hemilineages

305 (see Figure 3), or expression of Numb will make two Notch<sup>OFF</sup> hemilineages. In this way it will be possible to  
306 obtain RNAseq data on neurons with a common neuropil targeting program.

307 We used the cortex neurite length of neurons as a proxy for birth-order and shared temporal identity. We  
308 feel this is a good approximation (see Figure 5 for validation), but it clearly does not precisely identify  
309 neurons born during each of the Hb, Kr, Pdm, Cas temporal transcription factor windows. In the future,  
310 using genetic immortalization methods may allow long-term tracking of neurons that only transiently express  
311 each of these factors. Nevertheless, we had sufficient resolution to show that neurons within a temporal  
312 cohort (similar cortex neurite length) could target their pre- and post-synapses to distinct sub-domains of  
313 each hemilineage targeting domain. Because we have performed this analysis on segment A1 left in a single  
314 TEM reconstruction, it remains unknown whether the temporal identity sub-domains arise stochastically due  
315 to self-avoidance mechanism (41) or by using spacing cues (42, 43), or by precise responses to global  
316 patterning cues. Previous work in the mushroom body has shown how changes in temporal transcription  
317 factor expression can affect targeting, and in the optic lobe it has been shown how these changes can effect  
318 downstream axon pathfinding genes (43, 44). It is possible a similar mechanism could be functioning in the  
319 ventral nerve cord. Recent work has shown that manipulation of temporal identity factors in larval motor  
320 neurons can predictably retarget motor neuron axons in NB7-1(28). The first five divisions of NB7-1 dorsal  
321 hemilineage produces U1-U5 motor neurons which target the dorsal muscle field. Normally, progressively  
322 later born U motor neurons target progressively more ventral muscles, similar to the subregionalization we  
323 observe in the central nervous system. Mis-expression Hb can collapse all five U motor neuron axons to a  
324 single muscle target suggesting that, like the mushroom body, temporal transcription factors exert control  
325 over axon targeting programs. These results offer exciting parallels to what we observe in the ventral nerve  
326 cord, and suggest clear experiments to test the role of temporal factors in subregionalization of hemilineage  
327 targeting.

328 Independent of the mechanism, our results strongly suggest that hemilineage identity and temporal  
329 identity act combinatorially to allow small pools of 2-6 neurons to target pre- and post-synapses to highly  
330 precise regions of the neuropil, thereby restricting synaptic partner choice. Hemilineage information provides  
331 coarse targeting, whereas temporal identity refines targeting within the parameters allowed by hemilineage  
332 targeting. Thus, the same temporal cue (e.g. Hb) could promote targeting of one pool of neurons in one  
333 hemilineage, and another pool of neurons in an adjacent hemilineage. This limits the number of regulatory  
334 mechanisms needed to generate precise neuropil targeting for all ~600 neurons in a segment of the CNS.

335 In this study we demonstrate how developmental information can be mapped into large scale  
336 connectomic datasets. We show that lineage information, hemilineage identity, and birth order information  
337 can all be accurately predicted using morphological features. This both greatly accelerates the ability to  
338 identify neurons in a large EM volume as well as sets up a framework in which to study development using  
339 datasets typically intended for studying connectivity and function. While the work presented here explores  
340 how mechanisms known to be involved in generating neural diversity can also contribute to the establishment  
341 of axon targeting and neuropil organization, in the future we hope to utilize this dataset to explore how these  
342 developmental mechanisms correlate with connectivity and function. It is likely that temporally distinct  
343 neurons have different connectivity due to their sub-regionalization of inputs and outputs, however testing  
344 how temporal cohorts of neurons are organized into circuits remains an open question.

## 345 346 **Methods summary**

347  
348 For detailed methods see Supplemental File 1. Fly stocks are mentioned in the text and described in more  
349 detail in the Supplemental Methods. We used standard confocal microscopy, immunocytochemistry and



350 MCFO methods (24, 45, 46). When adjustments to brightness and contrast were needed, they were applied to  
351 the entire image uniformly. Mosaic images to show different focal planes were assembled in Fiji or  
352 Photoshop. Neurons were reconstructed in CATMAID as previously described (15, 24, 47). Analysis was  
353 done using MATLAB. Statistical significance is denoted by asterisks: \*\*\*\* $p < 0.0001$ ; \*\*\* $p < 0.001$ ; \*\* $p < 0.01$ ;  
354 \* $p < 0.05$ ; n.s., not significant.

355

### 356 **Acknowledgements**

357 We thank Haluk Lacin for unpublished fly lines. We thank Todd Lavery, Gerry Rubin, and Gerd Technau  
358 for fly stocks; Luis Sullivan, Emily Sales and Tim Warren for comments on the manuscript; Avinash  
359 Khandelwal and Laura Herren for annotating neurons; Keiko Hirono for generating transgenic constructs;  
360 and Keiko Hirono, Rita Yazejian, and Casey Doe for confocal imaging. Stocks obtained from the  
361 Bloomington *Drosophila* Stock Center (NIH P40OD018537) were used in this study. Funding was provided  
362 by HHMI (CQD, BM, LM, AAZ), NIH HD27056 (CQD), and NIH T32HD007348-24 (BM).

363

364 **Figure 1. Individual neuroblast progeny project widely within the neuropil**

365 (A) Three mechanisms specifying neuronal diversity.  
366 (B) Single neuroblast clones generated with *dpn(FRT.stop)LexA.p65* in newly-hatched larvae. We recovered  $n > 2$   
367 clones for each lineage except NB4-1 whose lineage morphology is well characterized in (13); posterior view; scale  
368 bar, 20  $\mu\text{m}$ .  
369 (C) The corresponding neurons traced in the TEM reconstruction. Dashed lines, neuropil border.  
370 (D) Each clone has one or two fascicles at the site of neuropil entry (blue). Number of neurons per clone  
371 show below for A1L and A1R.  
372 (E) Quantification of fascicle number at neuropil entry by light and EM microscopy.  
373 (F,G) Seven neuroblast lineages traced in the TEM reconstruction; posterior view (F), lateral view (G).

374  
375 **Figure 2. Lineages generate two morphological distinct classes of neurons which project to dorsal**  
376 **and ventral regions of the neuropil.**

377 (A-F) NBLAST clustering for the indicated neuroblast progeny typically reveals two morphological groups  
378 (red/cyan) that project to dorsal or ventral neuropil; these are candidate hemilineages. Cluster cutoffs were set  
379 at 3.0 for all lineages.  
380 (G) Superimposition of all dorsal candidate hemilineages (red) and all ventral candidate hemilineages (cyan).  
381 (H) Dendrogram showing NBLAST results clustering neurons based on similar morphology. Clustered  
382 neurons were all from hemisegment A1L. Colored bars denote lineage identity.

383  
384 **Figure 3. Hemilineage identity determines axon projection targeting to dorsal or ventral neuropil**

385 (A-C) Wild type. Posterior view of three neuroblast lineages expressing GFP using single NB-Gal4 drivers (see  
386 methods for genetics). Note the projections to dorsal neuropil (red arrowhead) and ventral neuropil (cyan  
387 arrowhead). Insets, anterior view of A1-A8 segments. Note: NB7-4 makes neurons (cyan arrowhead) and glia  
388 (red arrowhead). Below: summaries. Blue channel is either FasII or Phalloidin.  
389 (D-F) Notch<sup>intra</sup> mis-expression. Posterior view of three neuroblast lineages expressing GFP and  
390 constitutively active Notch<sup>intra</sup>. Note loss of the ventral projections and expansion of dorsal projections (red  
391 arrowhead). Insets, anterior view of A1-A8 segments.  $n > 3$  for all experiments. Below: summaries.

392  
393 **Figure 4. Hemilineage identity determines synapse targeting to motor or sensory neuropil domains**

394 (A) Spatial distributions of motor inputs (purple) and sensory outputs (green) show segregation of sensory  
395 axons and motor dendrites. Plots are 1D kernel density estimates for dorsoventral or mediolateral axes.  
396 Purple dots represent a single post-synaptic site. Green dots represent a single pre-synaptic site scaled by the  
397 number of outputs from that presynaptic site.  
398 (B) Spatial distributions of pre-motor inputs (post-synaptic sites of any neuron with  $> 3$  synapses onto a  
399 motor neuron in segment A1), or post-sensory outputs (pre-synaptic sites of any neuron with  $> 3$  synapses  
400 with an A1 sensory neuron) show the dorsal/ventral segregation of sensory/motor processing is preserved  
401 one layer into the networks.  
402 (C) 2D kernel density estimates of all pre/post synaptic sites for pre-motor and post-sensory neurons outlines  
403 the regions of sensory (green) and motor (magenta) processing in the VNC.  
404 (D,E) Each lineage generates a sensory targeting hemilineage and a motor targeting hemilineage. 2D kernel  
405 density estimates of post-synaptic and pre-synaptic sites for four neuroblast hemilineages. Note the restricted  
406 domains, and how both pre- and post-synaptic sites remain in the same functional neuropil domain. Purple  
407 and green regions are the contour line denoting the greatest 40% of all pre-motor (purple) or post-sensory  
408 (green) synaptic densities.  
409 (F,G) Pre- (F,F') and post- (G,G') synaptic density maps for all hemilineages.

410 (H) Connectivity diagram showing sensory neurons preferentially connect to neurons in ventral hemilineages,  
411 while motor neurons preferentially connect to neurons in dorsal hemilineages. Edges represent fractions of  
412 outputs for sensory neurons, and fraction of inputs for motor neurons.

413 (I) Summary showing that lineages generate a sensory and a motor processing hemilineage in a Notch-  
414 dependent manner.

415

416 **Figure 5. Different hemilineages target synapses to distinct domains of motor or sensory neuropil**

417 (A,B) Presynaptic distributions of four hemilineages (A) or five ventral hemilineages (B) shown in posterior  
418 view. Dots represent single pre-synaptic sites with their size scaled by the number of outputs from a given  
419 pre-synaptic site.

420 (C,D) Postsynaptic distributions of four dorsal hemilineages (C) or five ventral hemilineages (D) shown in  
421 posterior view. Dots represent single postsynaptic sites.

422 (E) Neurons with similar synapse positions tend to be in the same hemilineage. Dendrogram clustering  
423 neurons based on combined synapse similarity. Combined synapse similarity was determined by calculating a  
424 similarity matrix for pre-synapses and post-synapses separately and then averaging similarity matrices.

425

426 **Figure 6. Mapping temporal identity in the TEM reconstruction: radial position is a proxy for  
427 neuronal birth-order**

428 (A) Schematic showing correlation between temporal identity and radial position. Posterior view.

429 (B-D) Immunostaining to show the radial position of Hb+ and Cas+ neurons at embryonic stage 16 (B),  
430 recombinereed *Hb:GFP* (C), or *cas-gal4 UAS-RFP* (D) newly-hatched larvae (L0).

431 (E) Single cell clones of either Hb or late-born neurons. Hb neurons were labeled using *hb-T2A-LexA* (see  
432 methods). Late-born neurons were labeled using *cas-Gal4; MCFO*. We use the term late-born as we can not  
433 rule Gal4 perdurance into neuroblast progeny born after Cas expression ends.

434 (F) Neurons identified in the TEM reconstruction that match those shown in E.

435 (G) All Hb+ and late-born neurons identified in the TEM reconstruction.

436 (H) Distribution of cortex neurite lengths for known Hb+ and late-born neurons shows that late-born  
437 neurons are further from the neuropil than Hb+ neurons.

438 (I) Left/right homologous pairs of neurons with verified birthdates show highly stereotyped cortex neurite  
439 lengths across two hemisegments. Solid red line represents a linear fit, with dotted red lines representing 95%  
440 CIs.  $R^2 = .87$ ,  $p = 1.4e-8$ .

441

442 **Figure 7. Birth order dependent subregionalization of neuropil targeting exhibited by NB3-3  
443 neurons.**

444 (A-C) Full 11 cell clone of NB3-3 in hemisegments A1L and A1R. Colors were assigned by dividing the  
445 lineage into two temporal cohorts on the basis of cortex neurite length with the exception of A08m, which  
446 has been shown previously to be born early.

447 (D) Plot of mean cortex neurite lengths across bilateral pairs of NB3-3 neurons. Colors are assigned by  
448 dividing the lineage into two temporal cohorts. Mean cortex neurite length for the lineage was  $18\mu\text{m}$ , with  
449 four neurons having less than the mean (cyan cells). A08m has a mean length greater than  $18\mu\text{m}$ , but has been  
450 shown previously to be early-born. Asterisks denote neurons with confirmed birthdates matching their color  
451 assignment. 6/7 previously birthdated neurons had cortex neurite lengths consistent with their birthdate.

452 (E) Postsynaptic similarity clustering of NB3-3 neurons shows two groups divided by temporal cohort.  
453 Postsynaptic distributions of these two populations of cells show a dorsoventral division consistent with their  
454 differential input from chordotonal neurons (early-born NB3-3 neurons) or proprioceptive sensory inputs  
455 (late-born NB3-3 neurons).

456 (F) Presynaptic similarity clustering of NB3-3 neurons again shows a clustering of early and late-born neurons  
457 with the exception of A08m. Presynaptic distributions of these two populations of cells show both a  
458 dorsoventral split in the VNC as well as differential target regions for the projection neurons in the brain.  
459

460 **Figure 8. Birth-order dependent subregionalization of hemilineage targeting is a feature across**  
461 **many lineages.**

462 (A-H) NB5-2 ventral hemilineage. (A) NB5-2 ventral hemilineage (cyan, early-born; magenta, late-born).  
463 (B) Cortex neurite lengths of neurons in the hemilineage. (C-D) Presynaptic distributions of neurons in NB5-  
464 2V colored by birth-order. Little separation in the dorsoventral or mediolateral axes in the VNC was  
465 observed, but early-born neurons project axons to the brain while late-born neurons do not. (E-F)  
466 Presynaptic (E) and postsynaptic (F) similarity clustering of NB5-2V neurons shows neurons of a similar  
467 birth-order have similar synaptic positions. (G-H) Presynaptic (G) and postsynaptic (H) similarity plotted  
468 against birth order similarity. Birth-order similarity was defined as the pairwise Euclidean distance between  
469 cell bodies divided by the greatest pairwise distance between two cell bodies in the same hemilineage. Solid  
470 lines represent linear fits while dotted lines represent 95% CIs.  
471 (I-L) NB5-2 dorsal hemilineage. (I) NB5-2 dorsal hemilineage (cyan, early-born; magenta, late-born). (J)  
472 Cortex neurite lengths of neurons in NB5-2D. (K-L) Presynaptic distributions of neurons in NB5-2D colored  
473 by birth-order. Little separation in A/P axis in the VNC was observed, early-born and late-born neurons  
474 segregate in the D/V and M/L axes. (M-N) Presynaptic (M) and postsynaptic (N) similarity clustering of  
475 NB5-2D neurons shows neurons of a similar birth-order have similar synaptic positions. (O-P) Presynaptic  
476 (O) and postsynaptic (P) similarity plotted against birth order similarity. Birth-order similarity was defined as  
477 the pairwise Euclidean distance between cell bodies divided by the greatest pairwise distance between two cell  
478 bodies in the same hemilineage. Solid lines represent linear fits while dotted lines represent 95% confidence  
479 interval. For NB5-2D, a significant relationship between postsynaptic targeting and birth-order was not  
480 observed.  
481 (Q) Presynaptic (blue) and postsynaptic (red) similarity plotted against birth order similarity across nine  
482 hemilineages. NB1-2V was excluded as it only contained two neurons. When examined separately, only one  
483 hemilineage (NB1-2D) did not show a significant relationship between presynaptic similarity and birth-order  
484 similarity, and only one hemilineage (NB5-2D) did not show a significant relationship between postsynaptic  
485 similarity and birth-order similarity. Solid lines represent linear fits, and dashed lines represent 95%  
486 confidence interval.  
487 (R) Summary showing hemilineage targeting setting up broad neuropil targeting and temporal information  
488 sub-regionalizing hemilineage targeting.  
489

490

491 **Fig. S1. NB2-1 has two hemilineages containing neurons with similar “looper” morphology**  
492 (A) NBLAST dendrogram showing two candidate hemilineages (red, cyan) and two outlier neurons. Note  
493 that all neurons are highly similar compared to those shown in Figure 2, raising the question of whether they  
494 are a single hemilineage.  
495 (B-B') NB2-1 lineage generates both Notch<sup>OFF</sup> neurons (cyan arrowhead) and Notch<sup>ON</sup> neurons (red  
496 arrowhead) as detected by the Notch reporter Hey. Thus, NB2-1 generates two hemilineages.  
497 (C-C') TEM reconstruction of the NB2-1 neurons and a schematic showing two hemilineages (red, cyan) and  
498 two outliers (green, magenta). While A02o and A02l fasciculate with the other A02 neurons in at least four  
499 hemisegments, we never generated a clone containing either, and therefore chose to exclude them from  
500 further analysis.

501  
502 **Fig. S2. Ventral hemilineages have projection neurons**  
503 The indicated neuroblast lineages traced in catmaid showing the dorsal (red) and ventral (cyan) predicted  
504 hemilineages. Note that the ventral (cyan) hemilineages contains significantly longer axons (ascending and  
505 descending projection neurons) compared to dorsal (red) hemilineage neurons consistent with what has been  
506 observed in larva (Truman, 2010).  $P = .0034$ , via 2-sided Wilcoxon rank sum test.

507  
508 **Fig. S3. Hemilineage identity determines synapse targeting to motor or sensory neuropil domains**  
509 2D kernel density estimates for all hemilineages not shown in Figure 4. Density maps are of post-synaptic and  
510 pre-synaptic densities for four neuroblast lineages. Note the restricted domains, and how both pre- and post-  
511 synaptic sites remain in the same functional neuropil domain. Green and magenta regions represent density  
512 estimates for the pre-motor and post-sensory neurons for segment A1.

513  
514 **Fig. S4. Known Hb+ or Cas+ neurons identified in the TEM reconstruction**  
515 Cyan: neurons known to be Hb+. Magenta, neurons known to be Cas+. Posterior view, midline, dashed line;  
516 inset, dorsal view, anterior up.

517  
518 **Fig. S5. Neurons with a common temporal identity project widely within the neuropil**  
519 (A-F) Skeletons of 6 lineages colored by inferred birth order (cyan, early-born) to (magenta, late-born).  
520 Posterior view, dorsal up.  
521 (G) Quantification of cortex neurite length in each neuroblast lineage.  
522 (H) Overlay of all six lineages; note the intermingling of early- and late-born neuronal projections.  
523 (I, J) Pre- or post-synapse distributions of neurons position labeled by neuronal temporal identity; note the  
524 intermingling of synapses from early- and late-born neurons.

525  
526 **Fig. S6. Neurons in a hemilineage have more similar synaptic targeting than neurons in a temporal cohort.**  
527  
528 (A) Combined synapse similarity clustering similar to Figure 5E. Neuron names are colored either by  
529 hemilineage or by temporal cohort. Note the lack of coherent clusters of temporally-related neurons from  
530 different hemilineages.  
531 (B) Mean combined synapse similarity of neurons from hemilineages or temporal cohorts. Mean similarity  
532 was calculated by randomly selecting pairs of neurons in the same hemilineage or the same temporal cohort  
533 100 times.  $p < .0001$  via 2-sided Wilcoxon rank sum test.

534

535 **References**

- 536
- 537 1. Jessell TM (2000) Neuronal specification in the spinal cord: inductive signals and transcriptional codes. *Nature*
- 538 *reviews. Genetics* 1(1):20-29.
- 539 2. McDonald JA, *et al.* (1998) Dorsoventral patterning in the Drosophila central nervous system: the vnd homeobox
- 540 gene specifies ventral column identity. *Genes Dev* 12(22):3603-3612.
- 541 3. Weiss JB, *et al.* (1998) Dorsoventral patterning in the Drosophila central nervous system: the intermediate
- 542 neuroblasts defective homeobox gene specifies intermediate column identity. *Genes Dev* 12(22):3591-3602.
- 543 4. Isshiki T, Takeichi M, & Nose A (1997) The role of the msh homeobox gene during Drosophila neurogenesis:
- 544 implication for the dorsoventral specification of the neuroectoderm. *Development (Cambridge, England)* 124(16):3099-
- 545 3109.
- 546 5. McDonald JA & Doe CQ (1997) Establishing neuroblast-specific gene expression in the Drosophila CNS:
- 547 huckebein is activated by Wingless and Hedgehog and repressed by Engrailed and Gooseberry. *Development*
- 548 *(Cambridge, England)* 124(5):1079-1087.
- 549 6. Skeath JB, Zhang Y, Holmgren R, Carroll SB, & Doe CQ (1995) Specification of neuroblast identity in the
- 550 Drosophila embryonic central nervous system by gooseberry-distal. *Nature* 376(6539):427-430.
- 551 7. Zhang Y, Ungar A, Fresquez C, & Holmgren R (1994) Ectopic expression of either the Drosophila gooseberry-
- 552 distal or proximal gene causes alterations of cell fate in the epidermis and central nervous system. *Development*
- 553 *(Cambridge, England)* 120(5):1151-1161.
- 554 8. Chu-LaGraff Q & Doe CQ (1993) Neuroblast specification and formation regulated by wingless in the Drosophila
- 555 CNS. *Science (New York, N.Y.)* 261(5128):1594-1597.
- 556 9. Isshiki T, Pearson B, Holbrook S, & Doe CQ (2001) Drosophila neuroblasts sequentially express transcription
- 557 factors which specify the temporal identity of their neuronal progeny. *Cell* 106(4):511-521.
- 558 10. Skeath JB & Doe CQ (1998) Sanpodo and Notch act in opposition to Numb to distinguish sibling neuron fates in
- 559 the Drosophila CNS. *Development (Cambridge, England)* 125(10):1857-1865.
- 560 11. Truman JW, Moats W, Altman J, Marin EC, & Williams DW (2010) Role of Notch signaling in establishing the
- 561 hemilineages of secondary neurons in Drosophila melanogaster. *Development (Cambridge, England)* 137(1):53-61.
- 562 12. Harris RM, Pfeiffer BD, Rubin GM, & Truman JW (2015) Neuron hemilineages provide the functional ground plan
- 563 for the Drosophila ventral nervous system. *eLife* 4.
- 564 13. Lacin H & Truman JW (2016) Lineage mapping identifies molecular and architectural similarities between the larval
- 565 and adult Drosophila central nervous system. *eLife* 5:e13399.
- 566 14. Kolodkin AL & Tessier-Lavigne M (2011) Mechanisms and molecules of neuronal wiring: a primer. *Cold Spring*
- 567 *Harbor perspectives in biology* 3(6).
- 568 15. Ohyama T, *et al.* (2015) A multilevel multimodal circuit enhances action selection in Drosophila. *Nature*
- 569 520(7549):633-639.
- 570 16. Doe CQ & Goodman CS (1985) Early events in insect neurogenesis. I. Development and segmental differences in
- 571 the pattern of neuronal precursor cells. *Developmental biology* 111(1):193-205.
- 572 17. Dumstrei K, Wang F, & Hartenstein V (2003) Role of DE-cadherin in neuroblast proliferation, neural
- 573 morphogenesis, and axon tract formation in Drosophila larval brain development. *The Journal of neuroscience : the official*
- 574 *journal of the Society for Neuroscience* 23(8):3325-3335.
- 575 18. Bossing T, Udolph G, Doe CQ, & Technau GM (1996) The embryonic central nervous system lineages of
- 576 Drosophila melanogaster. I. Neuroblast lineages derived from the ventral half of the neuroectoderm. *Developmental*
- 577 *biology* 179(1):41-64.
- 578 19. Schmid A, Chiba A, & Doe CQ (1999) Clonal analysis of Drosophila embryonic neuroblasts: neural cell types, axon
- 579 projections and muscle targets. *Development (Cambridge, England)* 126(21):4653-4689.
- 580 20. Schmidt H, *et al.* (1997) The embryonic central nervous system lineages of Drosophila melanogaster. II. Neuroblast
- 581 lineages derived from the dorsal part of the neuroectoderm. *Developmental biology* 189(2):186-204.
- 582 21. Lacin H & Truman JW (2016) Lineage mapping identifies molecular and architectural similarities between the larval
- 583 and adult Drosophila central nervous system. *eLife* 5:eLife.13399.
- 584 22. Birkholz O, Rickert C, Nowak J, Coban IC, & Technau GM (2015) Bridging the gap between postembryonic cell
- 585 lineages and identified embryonic neuroblasts in the ventral nerve cord of Drosophila melanogaster. *Biology open*
- 586 4(4):420-434.
- 587 23. Kohwi M, Lupton JR, Lai SL, Miller MR, & Doe CQ (2013) Developmentally regulated subnuclear genome
- 588 reorganization restricts neural progenitor competence in Drosophila. *Cell* 152(1-2):97-108.
- 589 24. Heckscher ES, *et al.* (2015) Even-Skipped(+) Interneurons Are Core Components of a Sensorimotor Circuit that
- 590 Maintains Left-Right Symmetric Muscle Contraction Amplitude. *Neuron* 88(2):314-329.

- 591 25. Wreden CC, *et al.* (2017) Temporal Cohorts of Lineage-Related Neurons Perform Analogous Functions in Distinct  
592 Sensorimotor Circuits. *Current biology : CB* 27(10):1521-1528.e1524.
- 593 26. Costa M, Manton JD, Ostrovsky AD, Prohaska S, & Jefferis GS (2016) NBLAST: Rapid, Sensitive Comparison of  
594 Neuronal Structure and Construction of Neuron Family Databases. *Neuron* 91(2):293-311.
- 595 27. Baumgardt M, *et al.* (2014) Global programmed switch in neural daughter cell proliferation mode triggered by a  
596 temporal gene cascade. *Developmental cell* 30(2):192-208.
- 597 28. Seroka AQ & Doe CQ (2019) The Hunchback temporal transcription factor determines motor neuron axon and  
598 dendrite targeting in *Drosophila*. *Development (Cambridge, England)*.
- 599 29. Merritt DJ & Whittington PM (1995) Central projections of sensory neurons in the *Drosophila* embryo correlate  
600 with sensory modality, soma position, and proneural gene function. *J Neurosci* 15(3 Pt 1):1755-1767.
- 601 30. Zlatic M, Landgraf M, & Bate M (2003) Genetic specification of axonal arbors: atonal regulates robo3 to position  
602 terminal branches in the *Drosophila* nervous system. *Neuron* 37(1):41-51.
- 603 31. Landgraf M, Jeffrey V, Fujioka M, Jaynes JB, & Bate M (2003) Embryonic origins of a motor system: motor  
604 dendrites form a myotopic map in *Drosophila*. *PLoS Biol* 1(2):E41.
- 605 32. Mauss A, Tripodi M, Evers JF, & Landgraf M (2009) Midline signalling systems direct the formation of a neural  
606 map by dendritic targeting in the *Drosophila* motor system. *PLoS Biol* 7(9):e1000200.
- 607 33. Zlatic M, Li F, Strigini M, Grueber W, & Bate M (2009) Positional cues in the *Drosophila* nerve cord: semaphorins  
608 pattern the dorso-ventral axis. *PLoS Biol* 7(6):e1000135.
- 609 34. Doe CQ (2017) Temporal Patterning in the *Drosophila* CNS. *Annu. Rev. Cell Dev. Biol.* 33:in press.
- 610 35. Kambadur R, *et al.* (1998) Regulation of POU genes by castor and hunchback establishes layered compartments in  
611 the *Drosophila* CNS. *Genes Dev* 12(2):246-260.
- 612 36. Fekete DM, Perez-Miguelsanz J, Ryder EF, & Cepko CL (1994) Clonal analysis in the chicken retina reveals  
613 tangential dispersion of clonally related cells. *Developmental biology* 166(2):666-682.
- 614 37. Mihalas AB & Hevner RF (2018) Clonal analysis reveals laminar fate multipotency and daughter cell apoptosis of  
615 mouse cortical intermediate progenitors. *Development (Cambridge, England)* 145(17).
- 616 38. Wong LL & Rapaport DH (2009) Defining retinal progenitor cell competence in *Xenopus laevis* by clonal analysis.  
617 *Development (Cambridge, England)* 136(10):1707-1715.
- 618 39. Yu YC, Bultje RS, Wang X, & Shi SH (2009) Specific synapses develop preferentially among sister excitatory  
619 neurons in the neocortex. *Nature* 458(7237):501-504.
- 620 40. Yoshikawa S, McKinnon RD, Kokel M, & Thomas JB (2003) Wnt-mediated axon guidance via the *Drosophila*  
621 Derailed receptor. *Nature* 422(6932):583-588.
- 622 41. Zipursky SL & Grueber WB (2013) The molecular basis of self-avoidance. *Annual review of neuroscience* 36:547-568.
- 623 42. Petrovic M & Hummel T (2008) Temporal identity in axonal target layer recognition. *Nature* 456(7223):800-803.
- 624 43. Kulkarni A, Ertekin D, Lee CH, & Hummel T (2016) Birth order dependent growth cone segregation determines  
625 synaptic layer identity in the *Drosophila* visual system. *eLife* 5:e13715.
- 626 44. Zhu S, *et al.* (2006) Gradients of the *Drosophila* Chinmo BTB-zinc finger protein govern neuronal temporal  
627 identity. *Cell* 127(2):409-422.
- 628 45. Clark MQ, McCumsey SJ, Lopez-Darwin S, Heckscher ES, & Doe CQ (2016) Functional Genetic Screen to  
629 Identify Interneurons Governing Behaviorally Distinct Aspects of *Drosophila* Larval Motor Programs. *G3*  
630 (*Bethesda*).
- 631 46. Syed MH, Mark B, & Doe CQ (2017) Steroid hormone induction of temporal gene expression in *Drosophila* brain  
632 neuroblasts generates neuronal and glial diversity. *eLife* 6.
- 633 47. Carreira-Rosario A, *et al.* (2018) MDN brain descending neurons coordinately activate backward and inhibit forward  
634 locomotion. *eLife* 7.
- 635
- 636

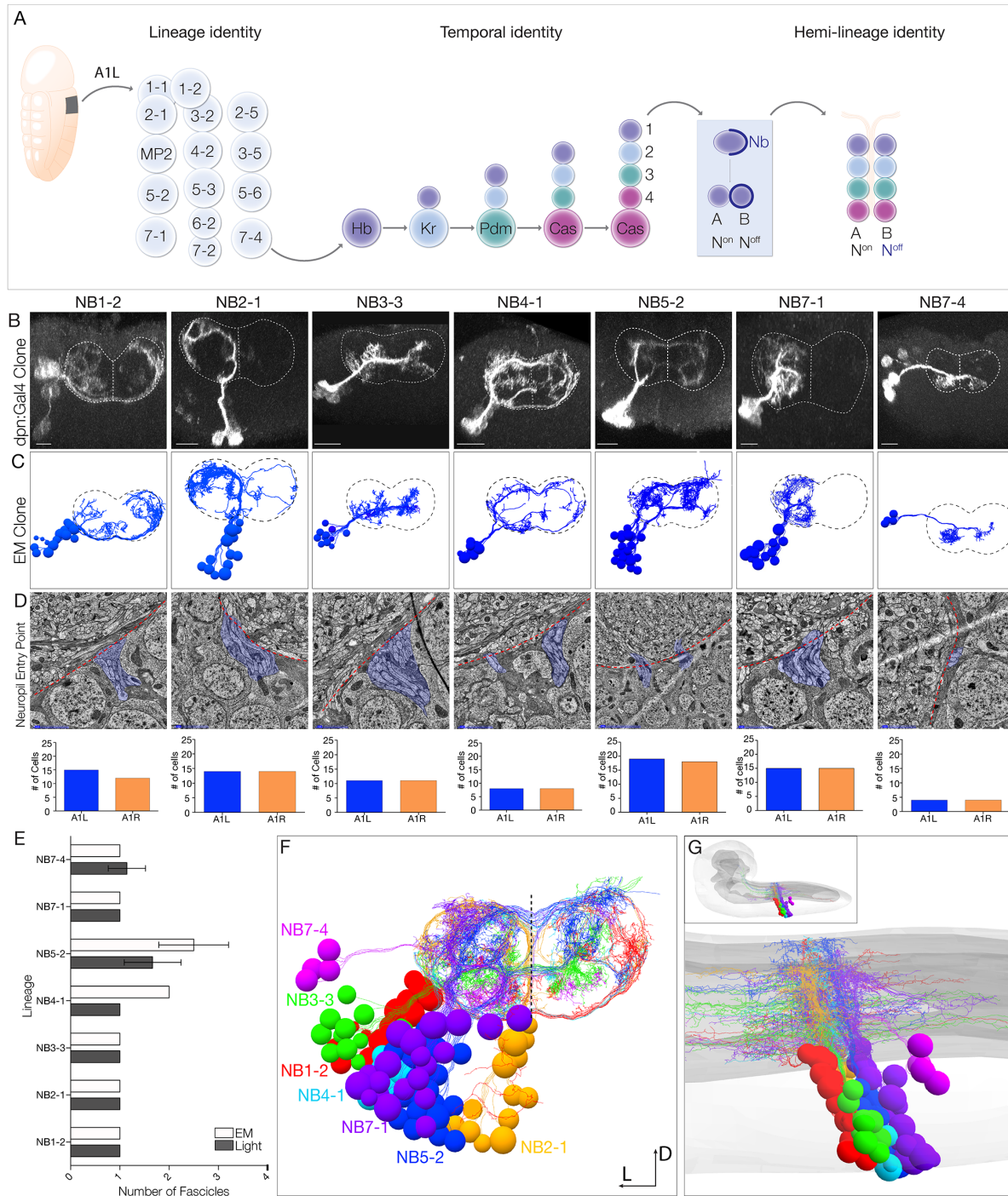


Figure 1

637



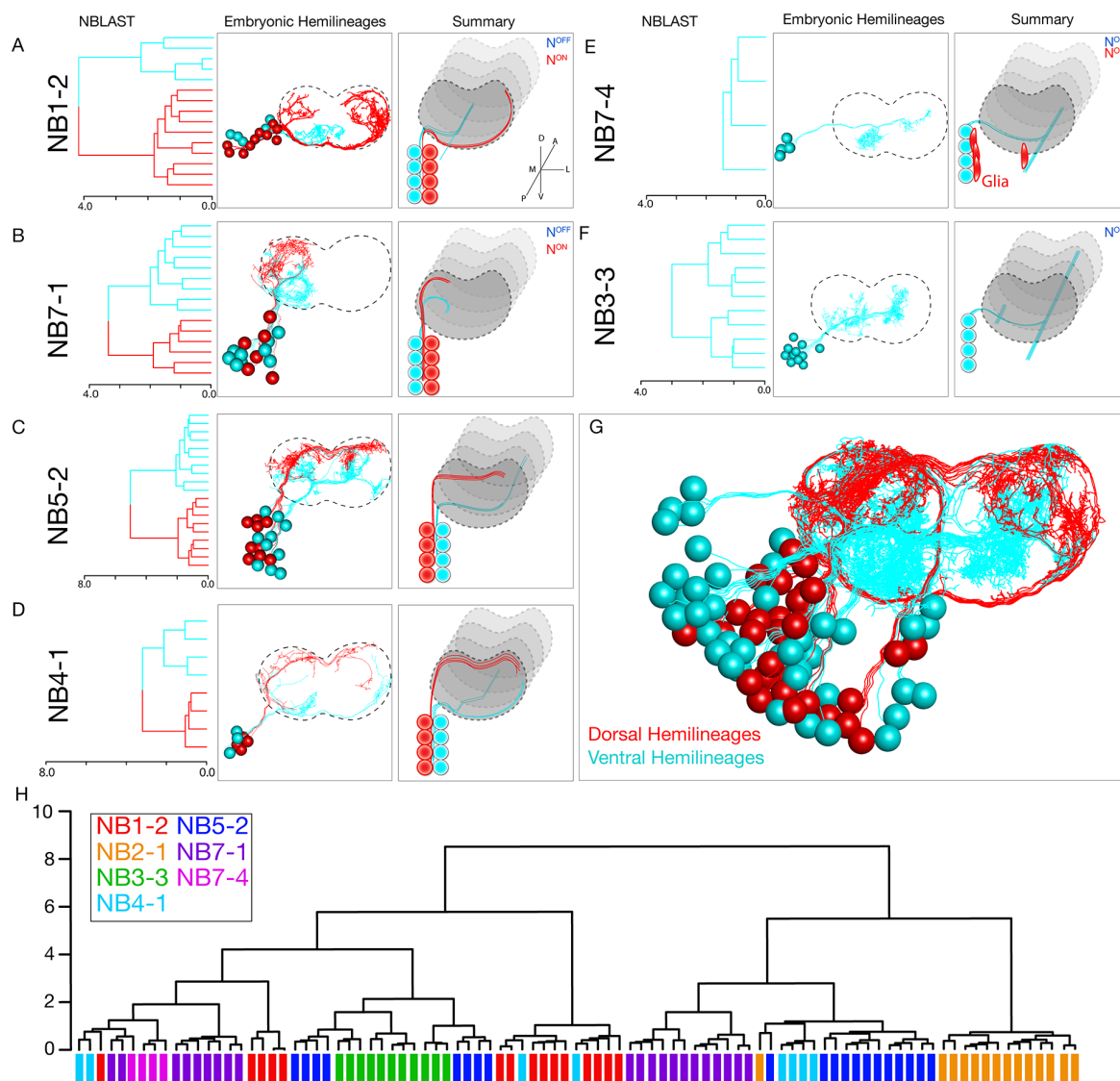


Figure 2

638

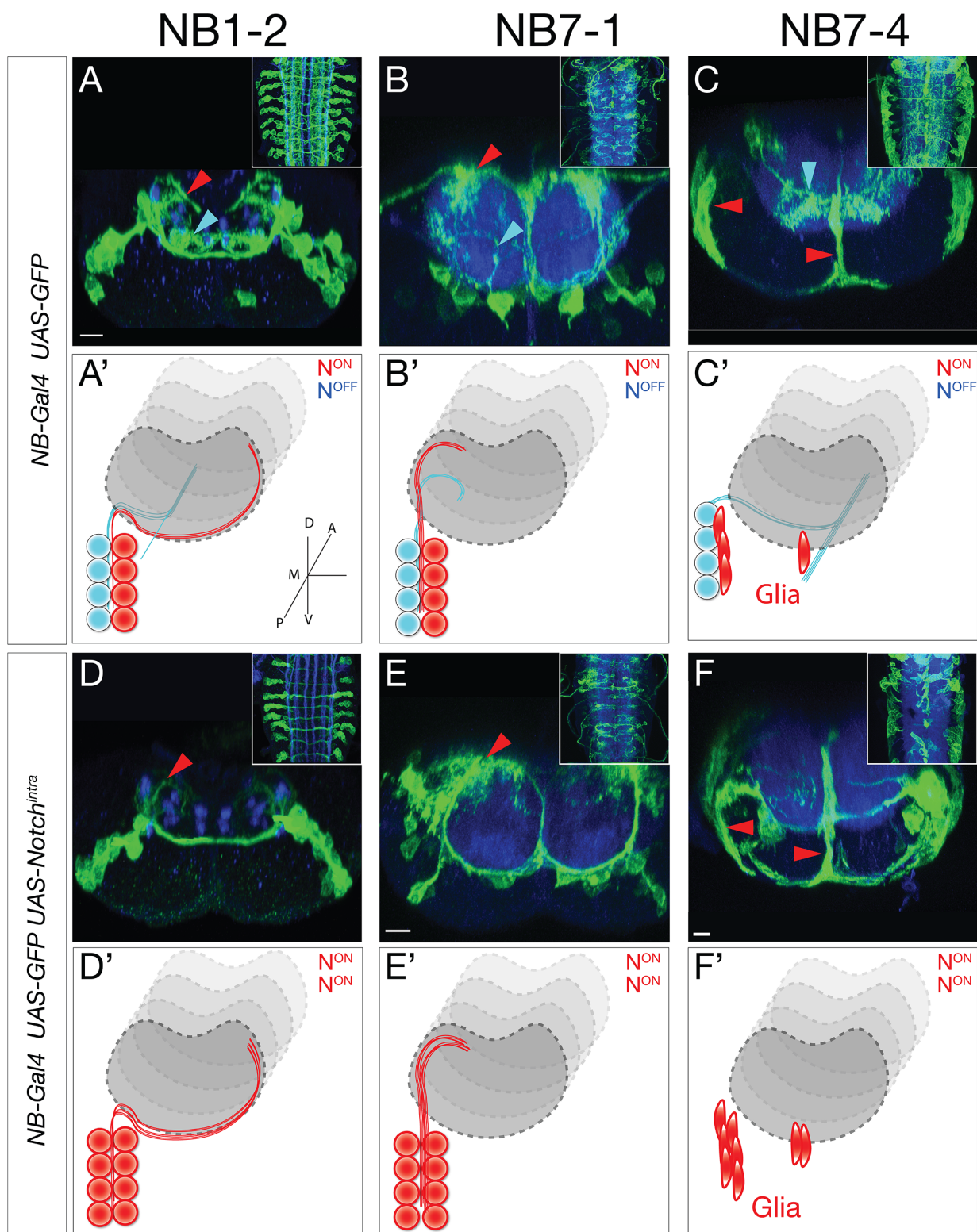
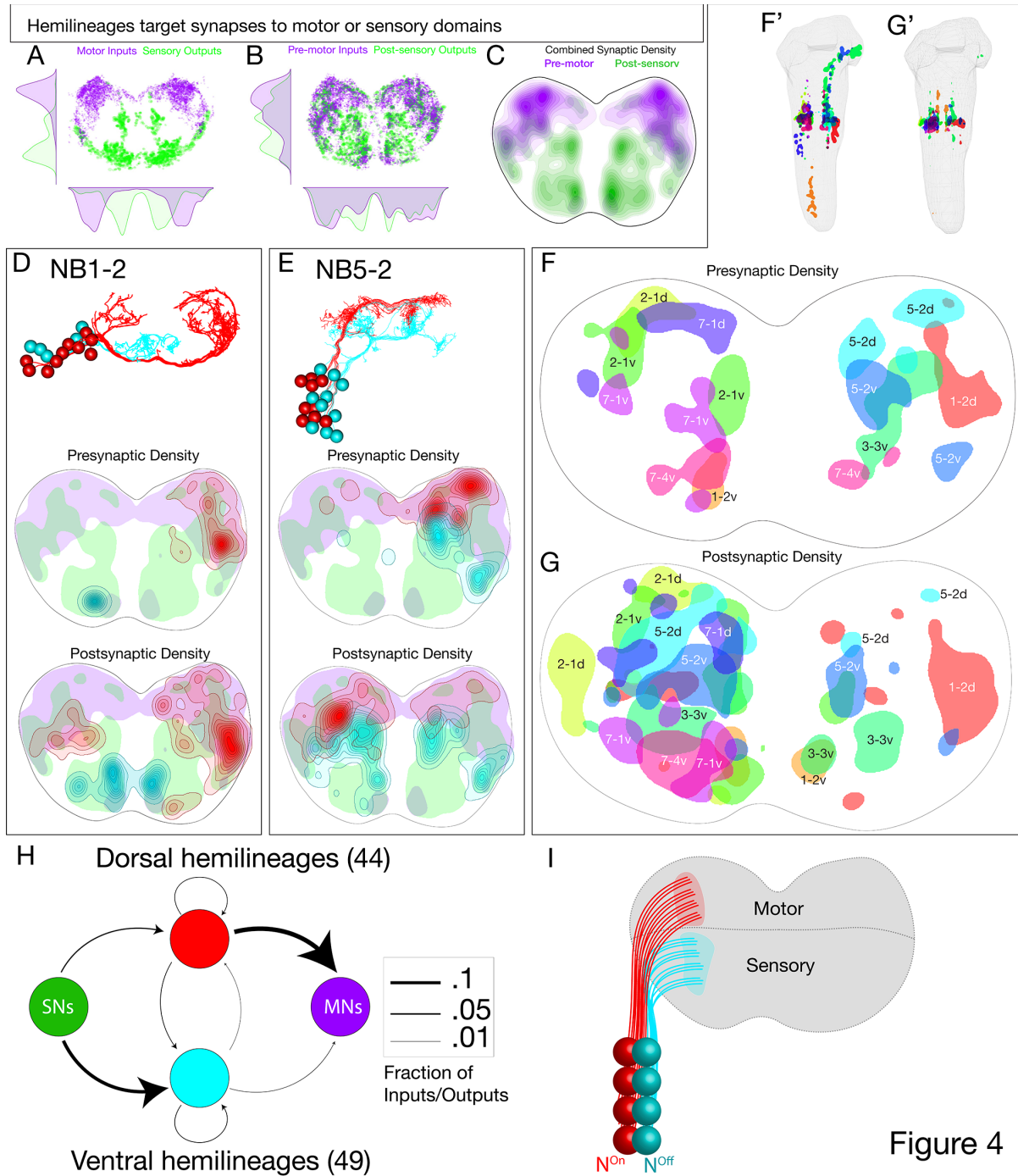
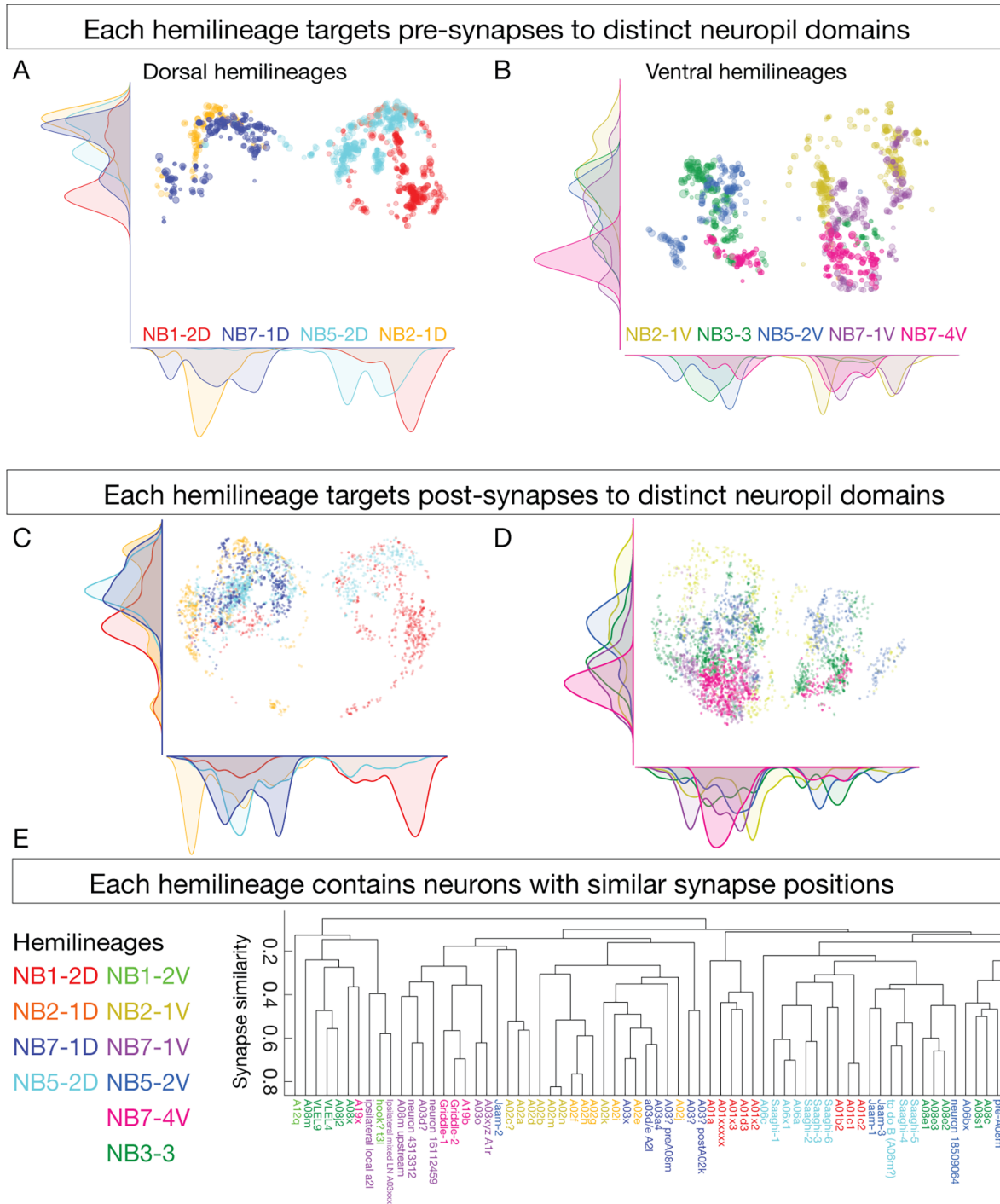


Figure 3

639



640



641

Figure 5

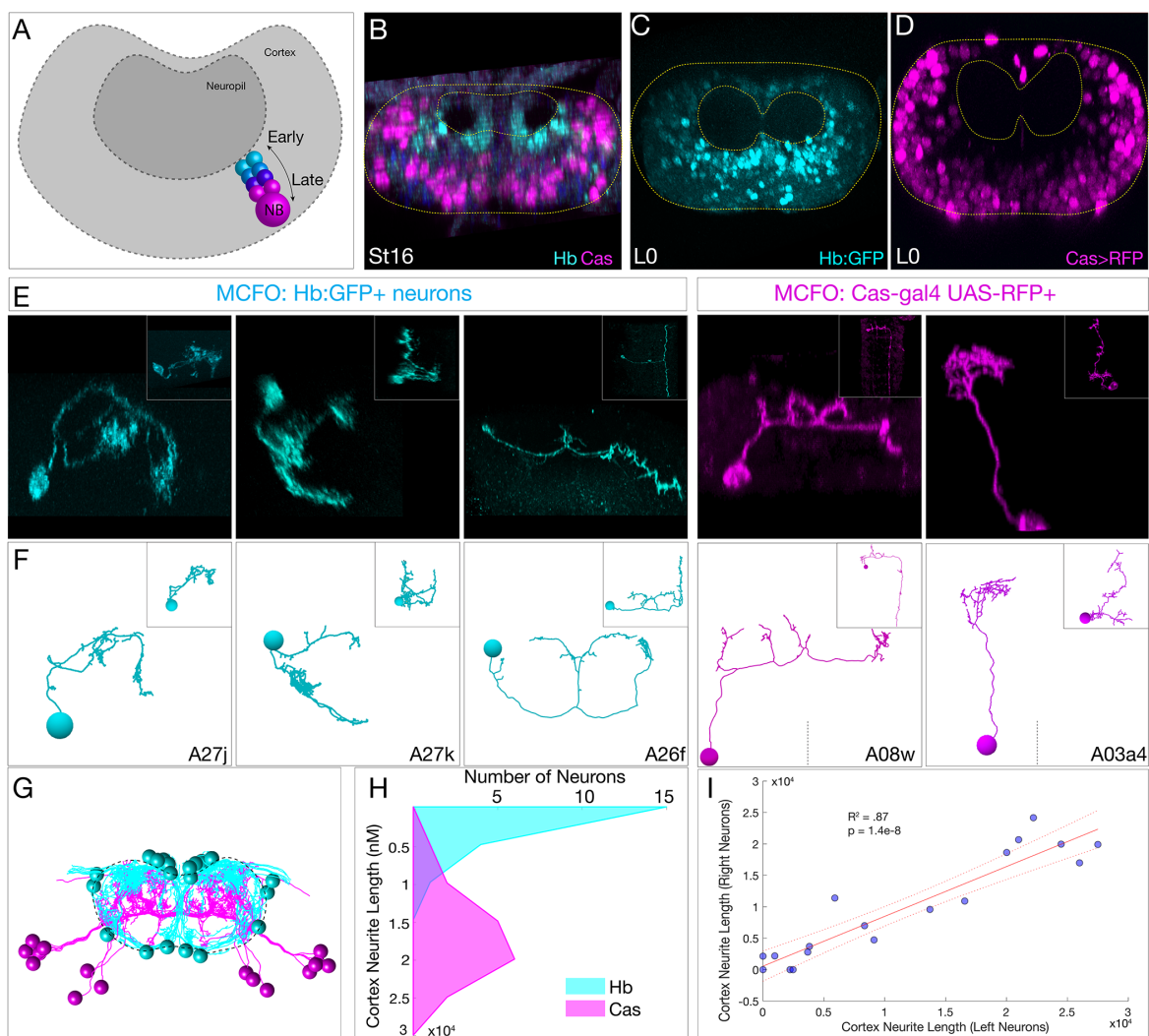


Figure 6

642

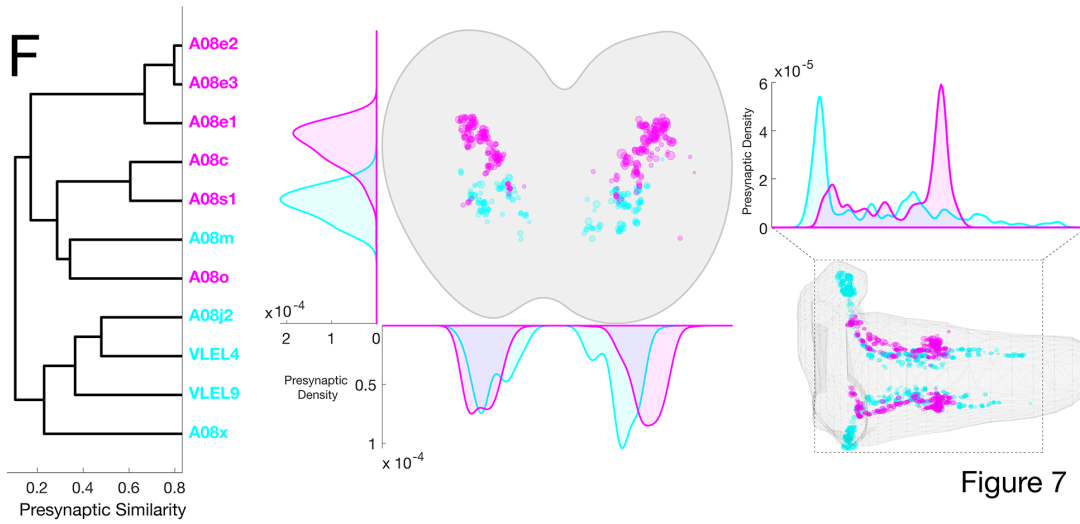
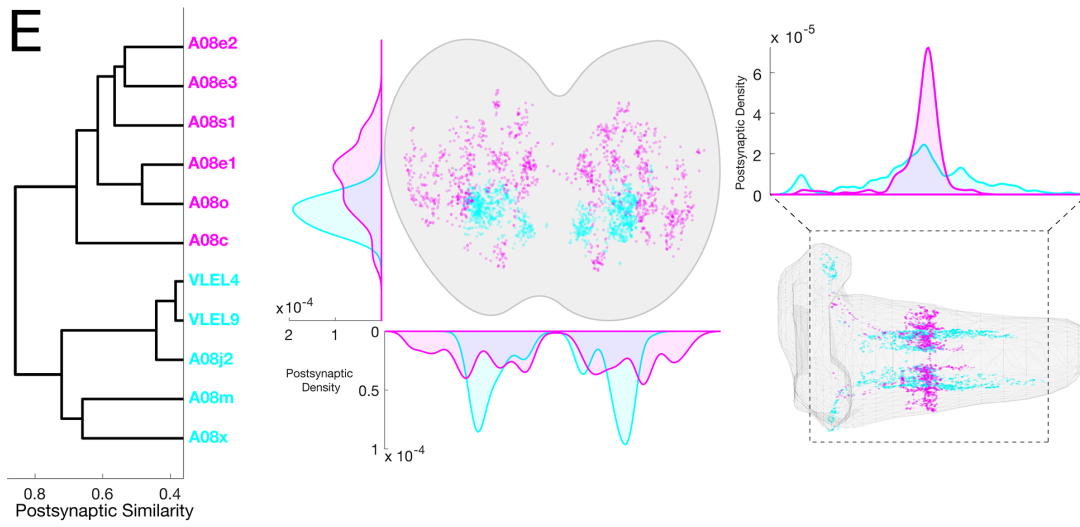
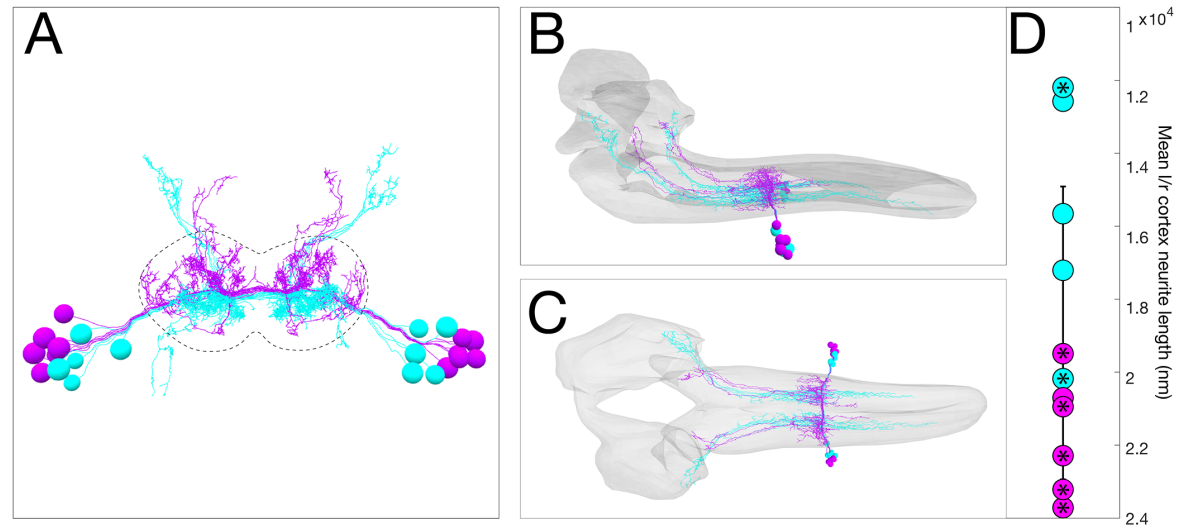
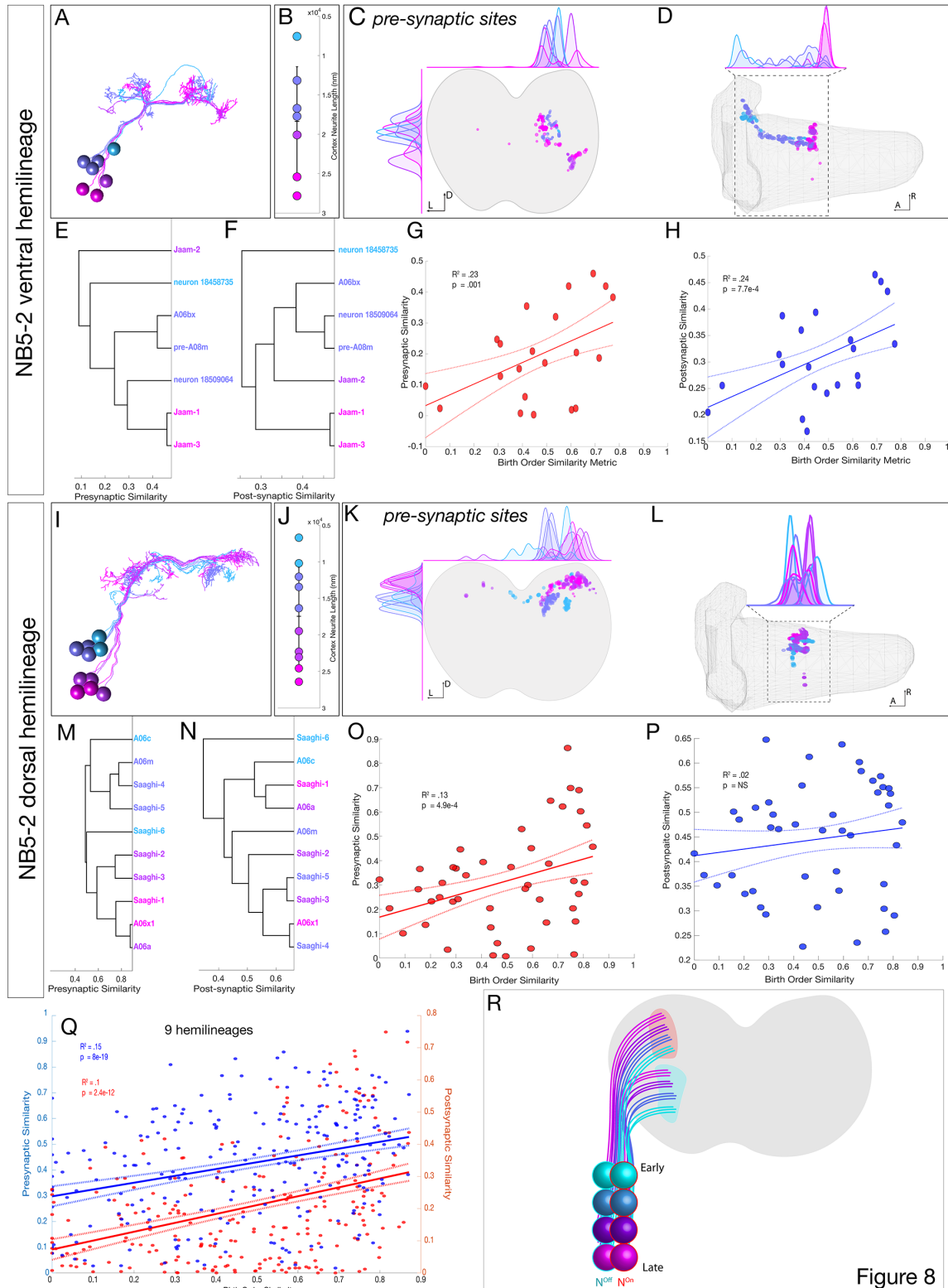
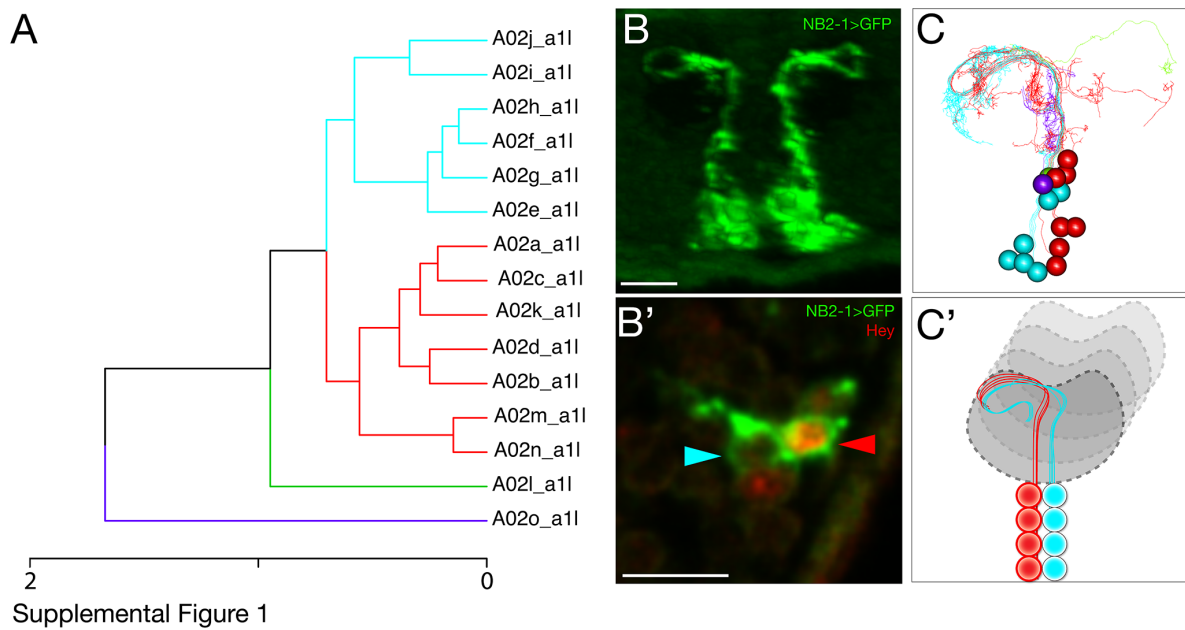


Figure 7

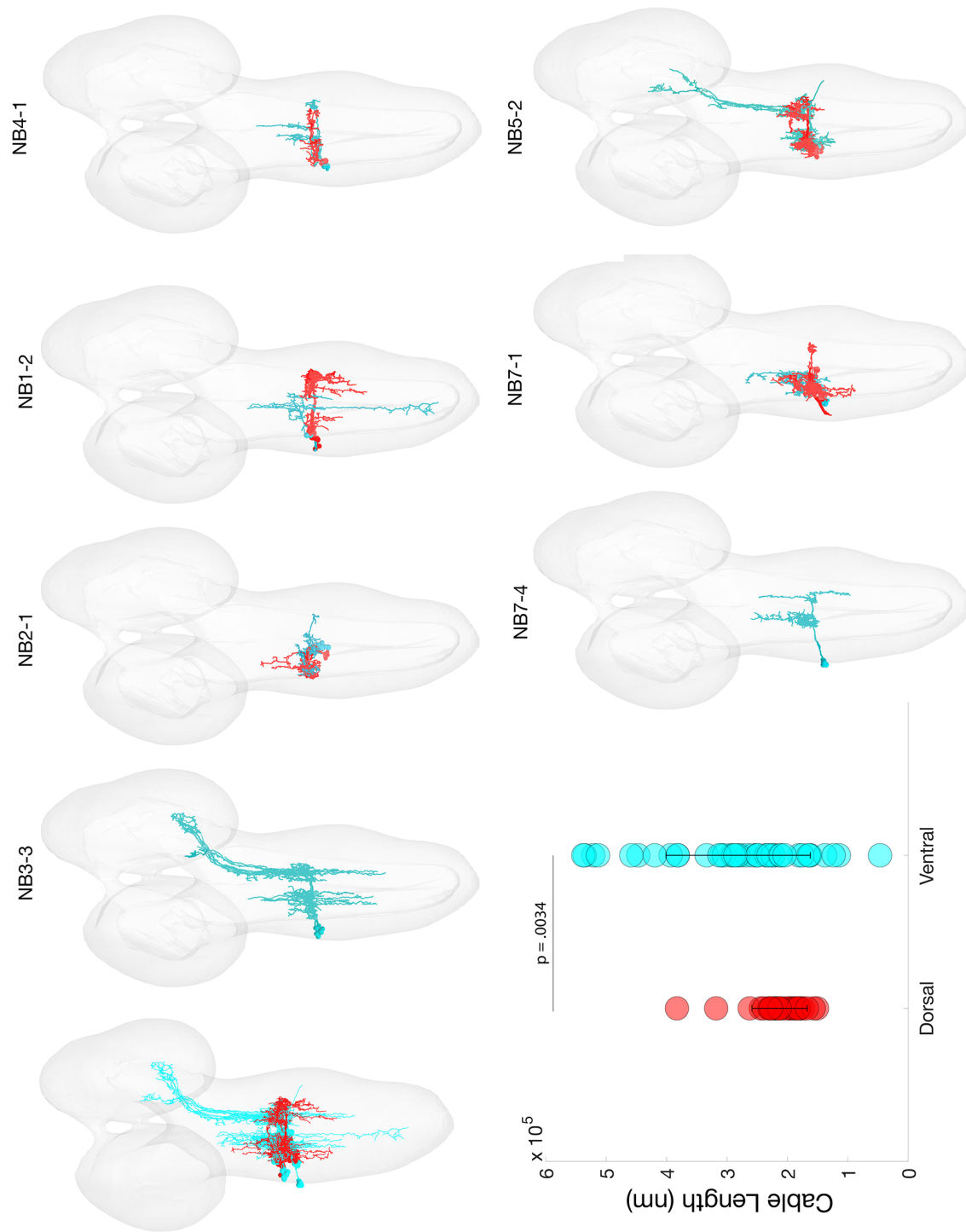
643





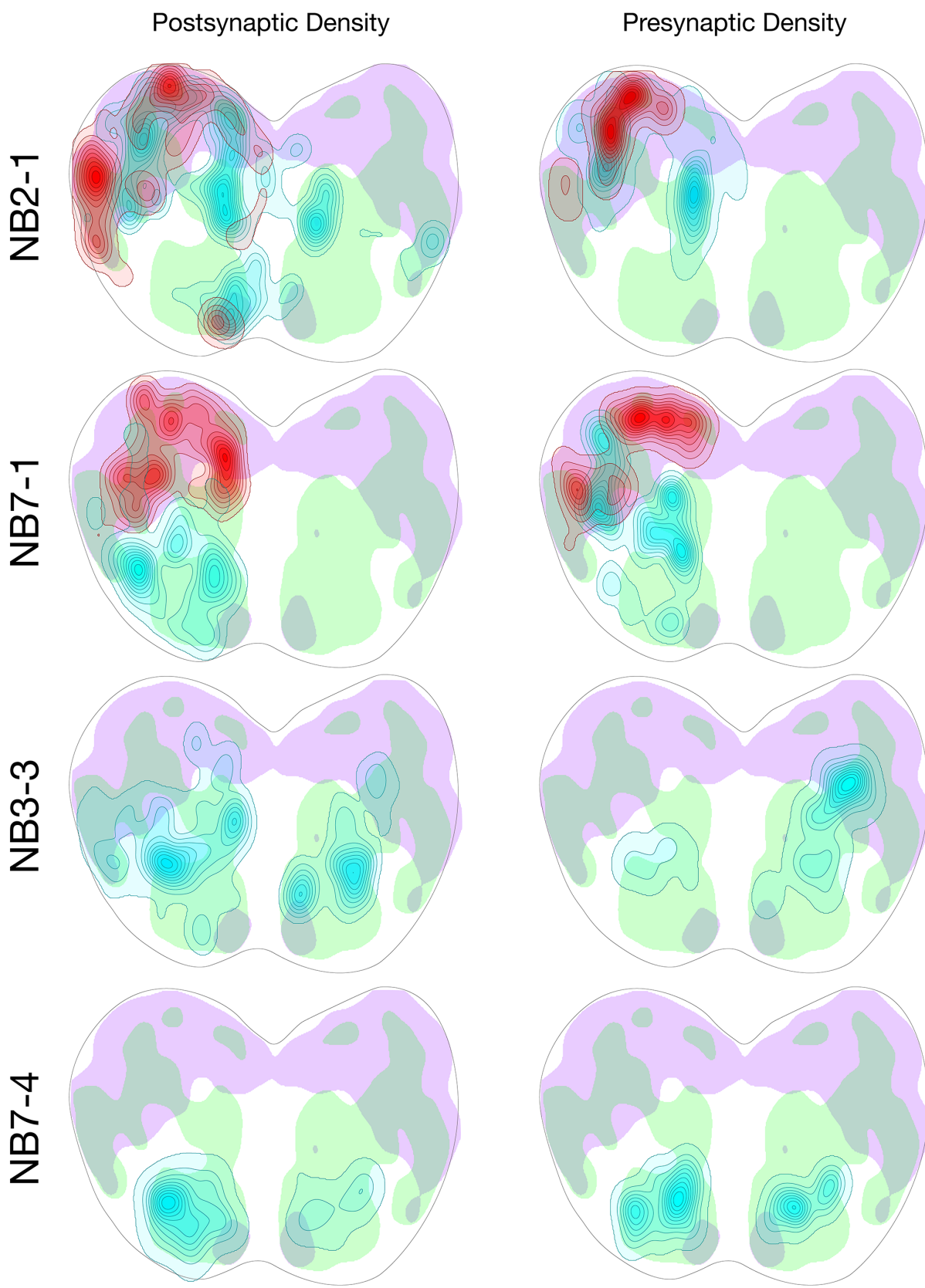
645

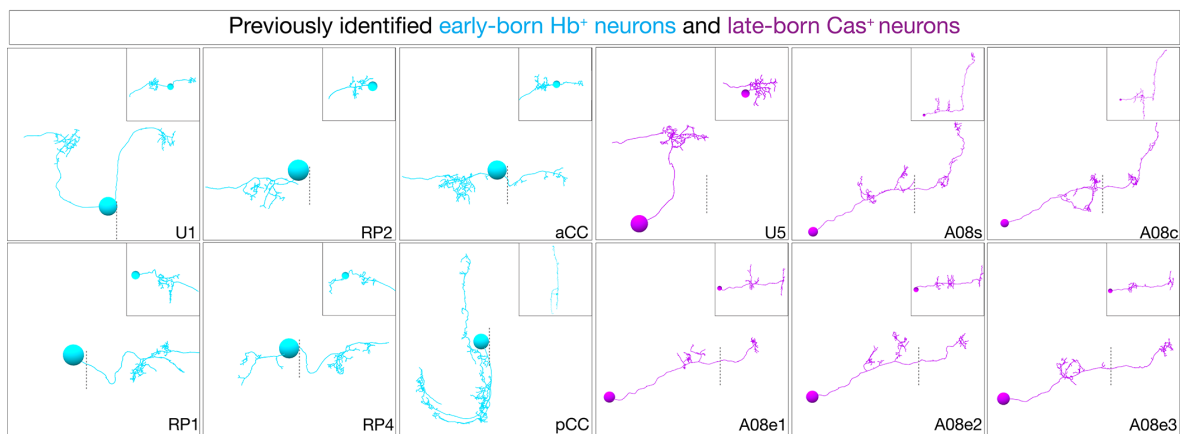




646

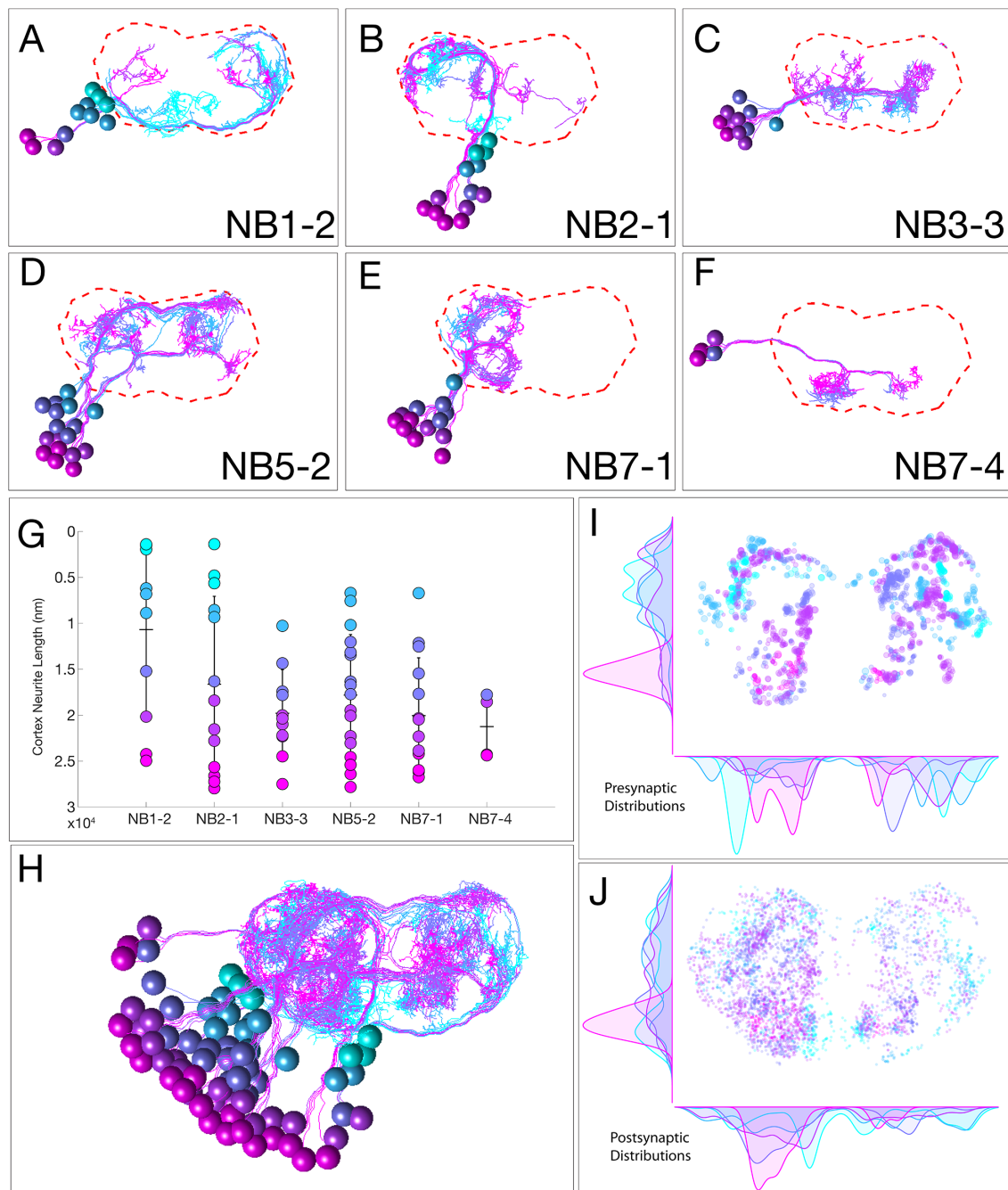
Supplemental Figure 2





648

Supplemental Figure 4



649

Supplemental Figure 5